Supporting Information

Cross-linkable Fullerene Derivatives for Solution-processed n–i-p Perovskite Solar Cells

Konrad Wojciechowski[1,†], Ivan Ramirez[1,†], Therese Gorisse[2], Olivier Dautel[3], Raghunath Dasari[4], Nobuya Sakai[1], Josue Martinez Hardigree[1], Seulki Song[5], Seth Marder[4], Moritz Riede[1], Guillaume Wantz[2], Henry J. Snaith[1,*]

† These authors contributed equally, * henry.snaith@physics.ox.ac.uk

Addresses

1. *Clarendon Laboratory, University of Oxford, Parks Road, OX1 3PU, United Kingdom*. 2. *IMS laboratory. Bordeaux Institute of Technology (IPB), University of Bordeaux, CNRS UMR 5218, ENSCBP, 16 Pey Berland, 33607 Pessac Cedex, France*. 3. *Institut Charles Gerhardt de Montpellier, Laboratoire AM2N, UMR CNRS 5253, ENSCM 8 rue de l'Ecole Normale, 34296 Montpellier, France.* 4. *School of Chemistry and Biochemistry and Center for Organic Photonics and Electronics, Georgia Institute of Technology, Atlanta, GA 30332, USA,* 5. *Department of Chemical Engineering, Pohang University of Science and Technology (POSTECH), San 31, Nam-gu, Pohang, Kyungbuk 790-784, Korea*

1. Experimental section

a) Materials and device fabrication

Unless otherwise stated, all materials were purchased from Sigma-Aldrich or Alfa Aesar and used as received. Fullerene (C_{60}), 99.5% purity was used. Spiro-OMeTAD was purchased from Borun Chemicals and used as received. The synthesis of the perovskite, $CH_3NH_3PbI_{3-x}Cl_x$ has been reported elsewhere.[1]

All the photovoltaic devices were fabricated on the fluorine-doped tin oxide (FTO)-coated glass substrates, supplied by Pilkington (TEC15 of 15 Ω/sq). The FTO coating was etched with zinc powder and 2M HCl. In order to achieve the desired pattern, areas where coating was not supposed to be etched were covered with stripes of scotch tape. The substrates were subsequently washed with Hellmanex solution (ca. 2 wt% in water), and then sonicated in acetone and isopropanol (IPA), 10 minutes in each solvent. Substrate preparation was completed with oxidising organic residues present on the FTO surface by piranha etching. The substrates were immersed in the piranha etch solution (sulphuric acid:hydrogen peroxide, 2:1 v/v), and heated at 150 °C for 2 hours. After the solution cooled down, the samples were thoroughly rinsed with deionised water, and sonicated in acetone and IPA. The optimised C_{60} compact layer was spin-coated on top of sintered FTO glass from the solution in 1,2-dichlorobenzene (10 mg/ml) at 1500 rpm, yielding in the film thickness of 37 nm, followed by drying at 60 °C for 2 minutes. The compact layer made of crosslinkable fulleropyrrolidine derivative containing triethoxysilane moiety (N-[3-(Triethoxysilyl)propyl]-2-carbomethoxy-3,4-fulleropyrrolidine, sol-gel C_{60}) was spin-coated on top of piranha-cleaned FTO substrate from the solution in 1,2-dichlorobenzene (concentration: 2, 4 or 6 mg/ml, spinning rate: 2000 rpm). After spin-coating the film was exposed to trifluoroacetic acid vapour for 60 seconds in order to trigger the crosslinking reaction. Then, the sample was transferred into a nitrogen-filled glovebox and annealed at 130 °C for 30 minutes to complete the crosslinking. After that time the sample was taken out of the glovebox and rinsed with methanol.. The electron collection layer made of the crosslinkable PCBM derivative, PCBCB, was spin-coated on top of piranha-cleaned FTO substrate from solution in 1,2-dichlorobenzene (concentration: 5 or 10 mg/ml, spinning rate: 2000 or 3000 rpm). After spin-coating, the sample was transferred into a nitrogen-filled glovebox and annealed at 200 °C for 10 minutes to crosslink the fullerene. Then, the sample was taken out of the glovebox and rinsed with methanol. The synthesis of the molecule was reported by Deb *et al.*[2] After the compact layer deposition samples were transferred into a nitrogen-filled glovebox. Perovskite precursor solution of the concentration of 380 mg/ml (CH_3NH_3I and $PbCl_2$, 3:1 molar ratio in dimethylformamide (DMF)) was spin-coated (spinning rate: 2000 rpm) at room temperature, followed by drying at room temperature for 30 min and annealing at 90 °C for 150 min, and 120 °C for 15 minutes, according to

the procedure reported elsewhere.[3] After the perovskite annealing process finished, surface passivation treatment was applied by spin-coating (spinning rate: 2000 rpm). a solution of iodopentafluorobenzene (IPFB) or thiophene on top of formed perovskite, as reported previously.[4,5] Subsequently, the hole transporter was deposited by spin-coating (spinning rate: 2000 rpm) a solution of 8 wt.% 2,2',7,7'-tetrakis-(N,N-di-pmethoxyphenylamine)9,9-spirobifluorene (spiro-OMeTAD, purchased from Lumtec or Borun Chemical) in chlorobenzene with added tert-butylpiridine (tBP) and lithium bis(trifluoromethanesulfonyl)imide (Li-TFSI) of 80 and 30 mol%, with respect to spiro-OMeTAD. Finally, 50 nm thick gold electrodes were deposited on top of devices by thermal evaporation at ~10^{-6} bar, through a shadow mask.

For perovskite PL measurements with different quenchers all the films were deposited on microscope glass substrates. The perovskite layers were then sealed with a ~100nm layer of the inert polymer poly(methylmethacrylate) (PMMA) (10 mg/ml, 1000 rpm) to reduce the impact of prolonged exposure to moisture.

b) Characterization techniques

Atomic Force Microscopy

Surface morphology was measured in air on a vibration-isolated Asylum Instruments MFP-3D atomic force microscope (AFM) in non-contact AC "tapping" mode in amplitude-feedback mode. Samples were scanned using BudgetSensors Tap 150Al-G Al-coated tips (force constant of 5 N/m, resonant frequency ~ 150 kHz). Soft-approach was used to reduce the possibility of surface-tip damage. A fast-axis scan rate of 0.6 Hz was used to ensure topographical features were accurately retraced. Histograms and image formatting were carried out using Gwyddion v2.45.[6]

Additional images were obtained using a ThermoMicroscope M5 in non-contact mode and scanning over a range of 5 μm by 5 μm at a resolution of 256 x 256 data points. The surface roughness was measured as the root mean-squared roughness over the scanning area.

Scanning Electron Microscopy

SEM images were obtained from a Hitachi S-4300 microscope.

Current voltage characteristics

JV characteristics of solar cells were measured under simulated AM1.5 100 $mW \cdot cm^{-2}$ sunlight (ABET Technologies Sun 2000) with a Keithley 2400 sourcemeter. The lamp was calibrated with an NREL-calibrated KG5 filtered silicon reference with a solar mismatch factor of 1.01. The active area of the device was defined by a metal mask with square aperture of the area of 0.0919 cm^2. The pre-masked active area of the solar cells was approximately 0.12 cm^2 nominally defined by the overlap area of the gold and FTO electrodes. Solar cells were masked for all the current voltage measurements.

Solar cells after encapsulation, before aging test were measured under simulated AM1.5 81.1 $mW \cdot cm^{-2}$ sunlight (calibrated with Fraunhofer KG5-filtered Si-reference cell, class AAA solar simulator).

Aging test was done at the maximum power point (MPP tracker), with a light intensity of 76.5 $mW \cdot cm^{-2}$, at the temperature of 60 °C, no active humidity control.

Photoluminescence Measurements

Time-resolved PL measurements were acquired using a time-correlated single photon counting (TCSPC) setup (FluoTime 300, PicoQuant GmbH). Film samples were photoexcited using a 507nm laser head (LDH-P-C-510, PicoQuant GmbH) pulsed at 1 MHz, with a pulse duration of 117 ps and fluence of 30 nJ/cm^2/pulse. The samples were exposed to the pulsed light source for ~10 minutes prior to measurement to ensure stable sample emission. The PL was collected using a high resolution monochromator and hybrid photomultiplier detector assembly (PMA Hybrid 40, PicoQuant GmbH).

UV-Vis absorption

UV-Vis absorption spectra were obtained using a Carry 300 Bio (Agilent Technologies) spectrometer in transmission mode.

SCLC

Electron mobilities were extracted using the Mott-Gurney law and a field-independent mobility. To ensure direct comparability with reported PCBCB values[2], the same PEDOT/fullerene/LiF/Al architecture was employed and Vbi taken to be 1.4 V.

2. Synthesis of sol-gel C_{60}[1]

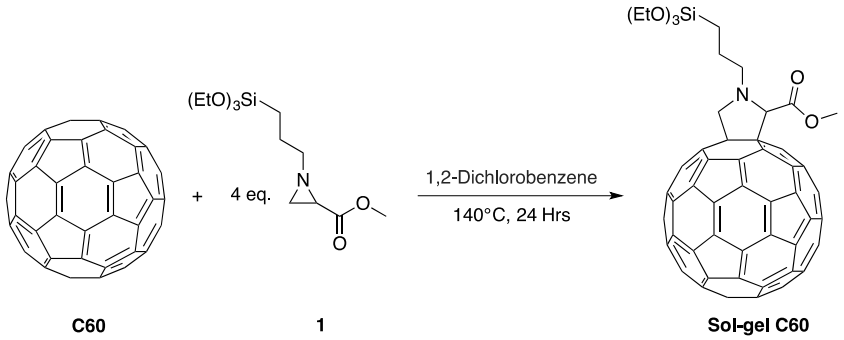

Figure S1. Schematic of the sol-gel C_{60} synthesis.

Materials. C_{60} was purchased from Sigma-Aldrich (99.5%). Methyl 2,3-dibromopropionate and all other reagents were used as purchased from Sigma-Aldrich. N-[3-(Triethoxysilyl)propyl]-2-carbomethoxy aziridine **1**[1] was synthesised as previously described starting from methyl 2,3-dibromopropionate. Toluene was purchased from Sigma-Aldrich and used without further purification. 1,2-dichlorobenzene was passed through alumina column and kept over molecular sieves.

N-[3-(Triethoxysilyl)propyl]-2-carbomethoxy-3,4-fulleropyrrolidine (**Sol-gel C_{60}**). 200 mg (0.14 mmol) of C_{60} were solubilised in 150 mL of 1,2-dichlorobenzene using an ultrasonic bath for 30 minutes. The blue solution was then degased through several vacuum-nitrogen cycles and 340 mg (1.12 mmol) of N-[3-(triethoxysilyl)propyl]-2-carbomethoxyaziridine (**1**) were added. After 24 h of heating at 140 °C, the solvent was removed in vacuo. The crude product was taken back into toluene (15 mL) and unreacted C_{60} separated by centrifugation. The supernatant was purified by gel permeation chromatography using polystyrene as stationary phase (Bio-Beads SX-3) and toluene as eluent (Figure S2). The faster eluting brown product is corresponding to the bigger and unsymmetrical **Sol-gel C_{60}** while unreacted C_{60} being smaller and symmetrical remained longer on the column to elute as the purple product. Using polystyrene gel instead of conventional silica gel allowed avoiding premature hydrolysis of the sol-gel C_{60} on the silica. The collected fractions were concentrated to 20 mL and 100 mL of EtOH were added to precipitate the fullerene derivative. 106 mg (37%) of sol-gel C_{60} were obtained after centrifugation. Sol-gel C_{60} was fully characterized by ^{1}H, ^{13}C and ^{29}Si NMR techniques. Analyses were in good accordance with the literature. ^{1}H NMR (400 MHz, $CDCl_3$): δ 0.85-1.10 (m, 2H), 1.29 (t, 9H, *J* = 6.8 Hz), 1.96- 2.16 (m, 2H), 2.94-3.04 (m, 1H), 3.31-3.39 (m, 1H), 3.86 (s, 3H), 3.90 (q, 6H, *J* = 6.8 Hz), 4.32, (d, 1H, *J* = 9.2 Hz), 5.08 (d, 1H, *J* = 9.2 Hz), 5.10 (s, 1H). ^{13}C NMR (100 MHz, $CDCl_3$): δ 8.19, 18.43, 21.71, 51.50, 52.27, 55.33, 58.54, 65.21, 69.57 (Csp3, fullerene), 72.76 (Csp3, fullerene), 77.73, 133.31, 135.44, 136.10, 136.60, 137.77, 139.73, 139.90, 140.28, 140.33, 141.85, 141.98, 142.04, 142.13, 142.16, 142.26, 142.28, 142.65, 142.68, 142.71, 143.10, 143.13, 144.48, 144.50, 144.58, 144.69, 145.30, 145.33, 145.36, 145.42, 145.44, 145.50, 145.66, 145.71, 145.81, 145.84, 146.08, 146.10, 146.25, 146.27, 146.32, 146.39, 147.34, 147.44, 151.13, 153.65, 154.75, 154.8, 170.54 (C=O). ^{29}Si NMR (79.5 MHz, $CDCl_3$): δ -45,35 (s, 1Si). FT-IR: ν 2972 ($\nu_{as}CH_3$), 2931 ($\nu_{as}CH_2$), 2882 (νCH_3), 2840 (νCH_2), 1755 (νC=O), 1736 (νC=O), 1434 (νC=C, fullerene), 1175 (ν_{as}C-OSi), 1103 (ν_{as}Si-OEt), 1078 (νSi-OEt), 955 (νC-OSi) cm^{-1}.

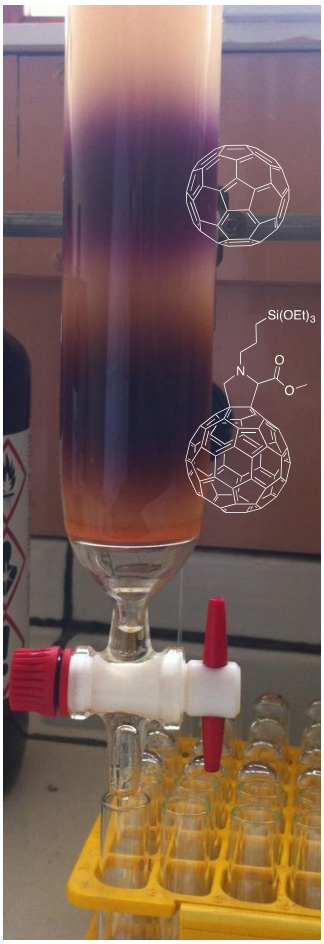

Figure S2. Purification of a mixture of **Sol-gel C_{60}** and unreacted C_{60} in toluene by gel permeation chromatography using polystyrene as stationary phase (Bio-Beads SX-3) and toluene as eluent.

The faster eluting brown product is corresponding to the bigger and unsymmetrical **Sol-gel C_{60}** while unreacted C_{60} being smaller and symmetrical remained longer on the column to elute as the purple product. Using polystyrene gel instead of conventional silica gel allowed avoiding premature hydrolysis of the sol-gel C_{60} on the silica.

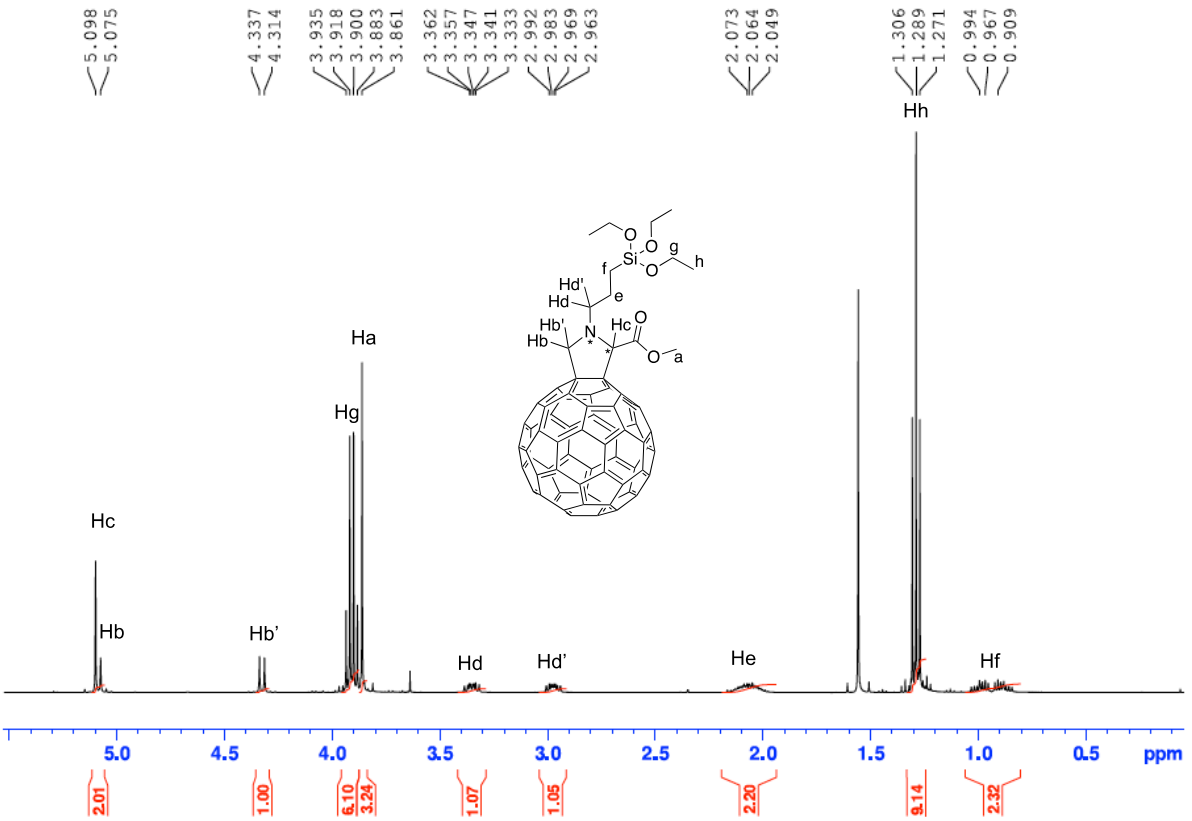

Figure S3. ^{1}H NMR spectrum of **Sol-gel C_{60}** recorded at 400 MHz in $CDCl_3$.

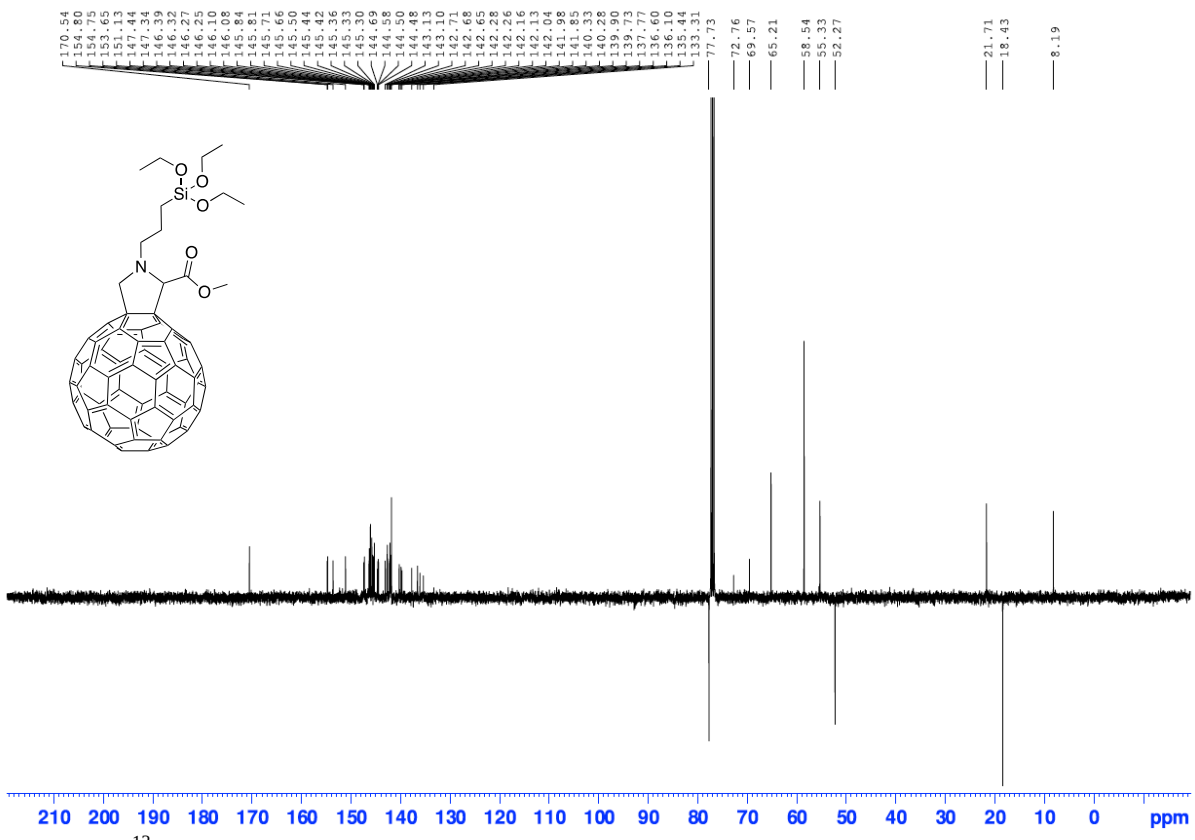

Figure S4. ^{13}C NMR spectrum of **Sol-gel C_{60}** recorded at 100 MHz in $CDCl_3$.

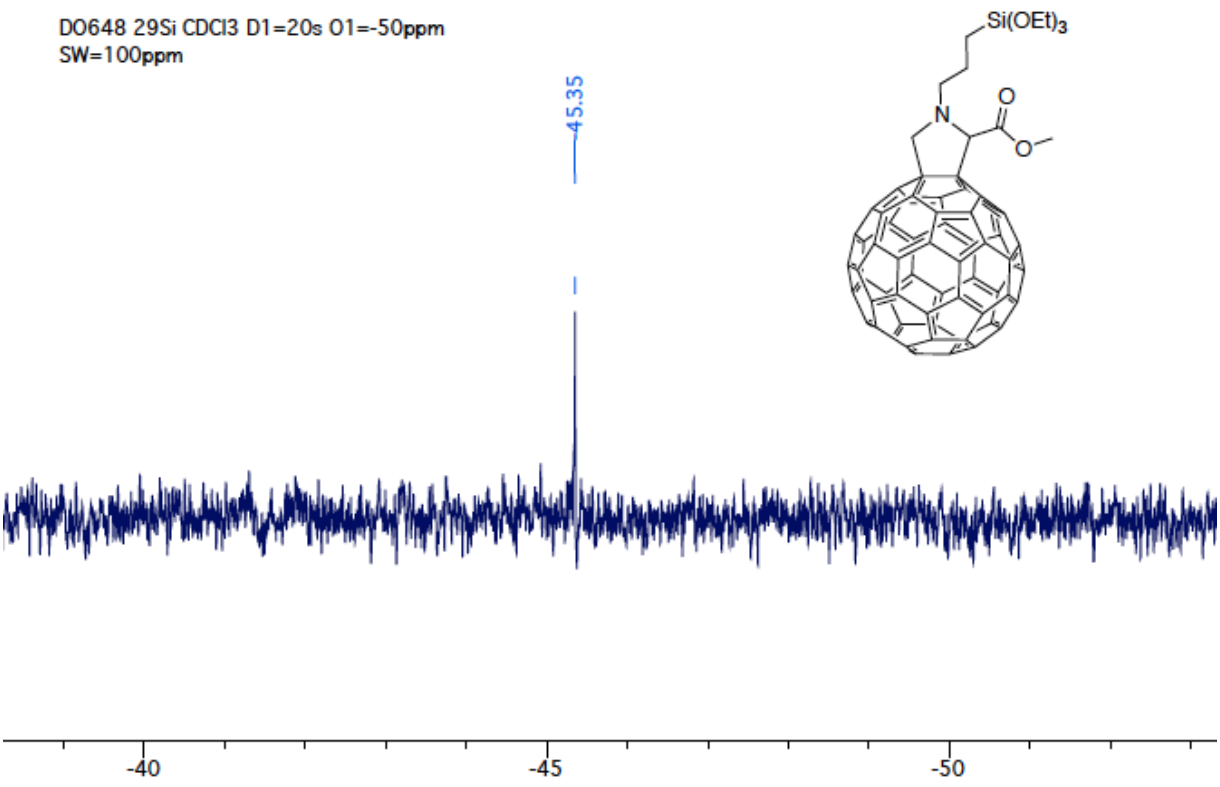

Figure S5. ^{29}Si NMR spectrum of **Sol-gel C_{60}** recorded at 79.5 MHz in $CDCl_3$.

3. Cross-linking of the sol-gel C_{60}

The transformation can be monitored in the sol-gel C_{60} FTIR spectrum (**Figure S6a**), from the band intensity of the asymmetric ($\nu_{as}CH_3$) and symmetric (ν_sCH_3) stretching vibrations of the CH_3, at 2973 and 2882 cm^{-1}, respectively. In the sol-gel C_{60}/TFA spectrum these bands completely disappear which is significant of the hydrolysis of the Si-OEt bonds. Similarly, formation of the Si-O-Si network can be followed by the decrease of the band intensity of the asymmetric (ν_{as}Si-O-Et, 1103 cm^{-1}) and symmetric (ν_sSi-O-Et, 1078 cm^{-1}) stretching vibrations of the Si-OEt bond, the decrease of the band intensity of the asymmetric (ν_{as}C-OSi, 1170 cm^{-1}) and symmetric (ν_aC-OSi, 955 cm^{-1}) stretching vibrations of the CH_3CH_2C-OSi bond, and the appearance of the broad band from 980 to 1255 cm^{-1} corresponding to the asymmetric and symmetric stretching vibrations of various Si-O-Si bonds of the silicate network. After TFA vapour exposure, absorption bands corresponding to the acid can be observed in the sol-gel C_{60}/TFA spectrum, with the vibration of the carbonyl (νC=O, 1784 cm^{-1}), C-O

(1210 cm^{-1}), and C-F (1175 cm^{-1}) functions. Accordingly, residual Si-OH functions (νSiO-H, around 3400 cm^{-1}, Figure S6a) can be monitored, indicating the level of completion of the condensation process. The removal of the TFA traces and complete condensation is achieved after 30 minutes of thermal annealing at 130 °C in a nitrogen-filled glovebox. This is confirmed by the disappearance of the vibrations corresponding to the TFA (νC=O, νC-O, νC-F), and the one corresponding to the silanol (νSiO-H) in the sol-gel C_{60}/TFA/130 °C spectrum.

a)

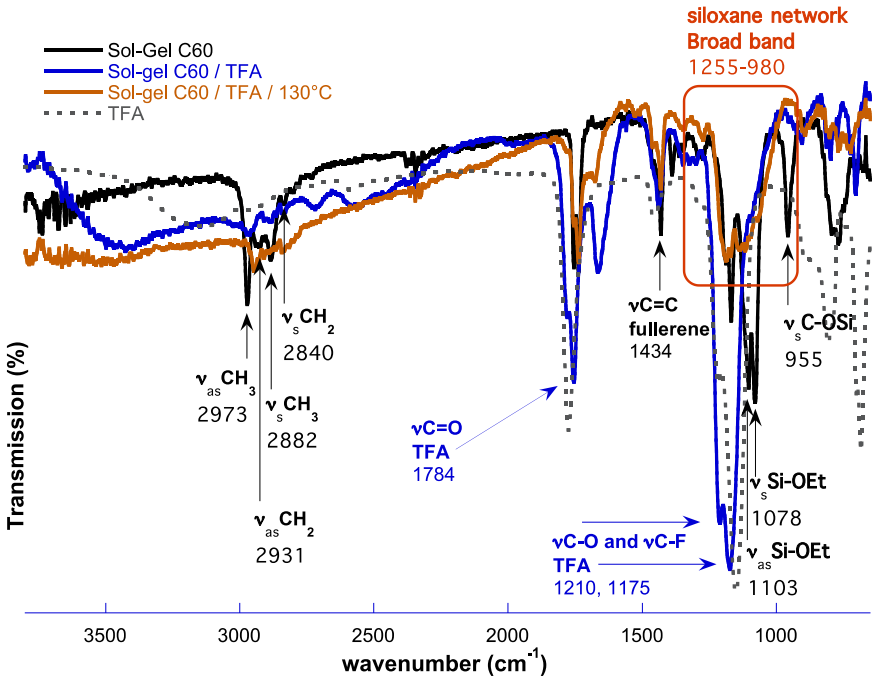

b)

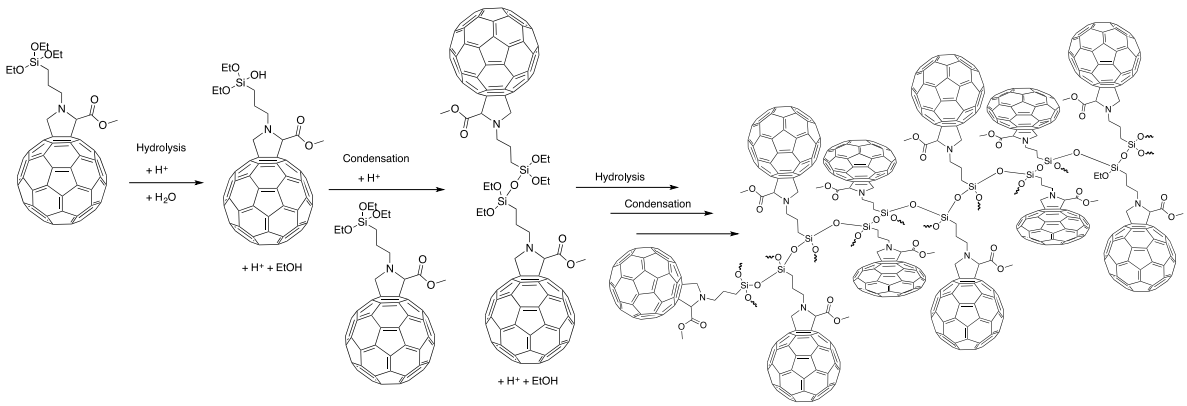

Figure S6. (a) FT-IR spectrum of a spin-coated thin film of sol-gel C_{60} on a silicon wafer from a chlorobenzene solution, before exposure to TFA vapour (black curve), after exposure to TFA vapour (blue curve), and after exposure to TFA vapour followed by a thermal annealing at 130 °C (red curve). The grey dashed curve is corresponding to the FT-IR spectrum of pure TFA; **(b)** schematic of a hybrid network generated by the acid-catalysed hydrolysis and polycondensation of the sol-gel C_{60}.

4. Estimation of the LUMO levels by cyclic voltammetry

The LUMO level of sol-gel C60 in solution was measured by cyclic voltammetry measurements. We highlight that these energy levels are bound to be different to those of films, which change again upon cross-linking. Pt wires were used as working and counter electrodes and an Ag wire as pseudo reference electrode. The analysis were performed on a 10^{-3}M solution of **Sol-gel C_{60}** in an electrolyte (0.1 M Bu_4NPF_6 in tetrahydrofuran solution) at room temperature with a scan rate of 100 mV/s and ferrocenium/ferrocene (Fc^+/Fc) redox couple as external reference ($E_{Fc+/Fc}$ = 0.4 V/SCE). The cyclic voltammogram of sol-gel C60 and PCBM (as a comparison) are shown in figure S7. The LUMO level has been deduced from the reduction onset of the sol-gel C60 under the assumption that the energy level of Fc is 4.7 eV below vacuum level.[2]

$$E_{ox}\text{onset Fc} = 0.3\text{ V}, E_{red}\text{onset sol-gel } C_{60} = -0.55\text{ V}$$

$$E_{LUMO}\ \textbf{sol-gel } \boldsymbol{C_{60}} = -(4.7-(0.55+0.3)) = -3.85\ eV$$

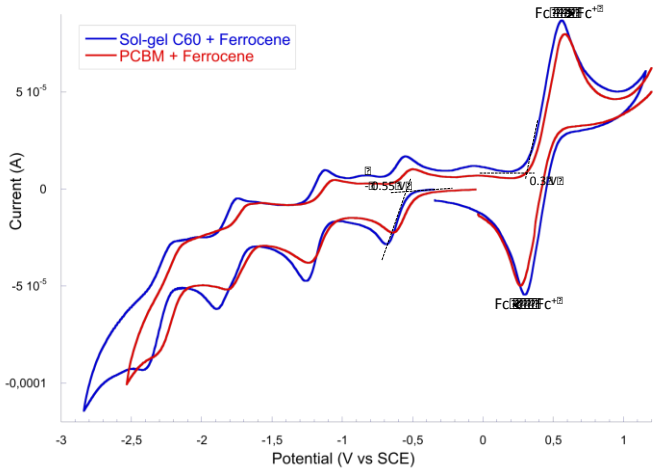

Figure S7. Cyclic voltammogram of a 10^{-3}M solution of Sol-gel C_{60} in an electrolyte (0.1 M Bu_4NPF_6 in tetrahydrofuran solution) at room temperature with a scan rate of 100 mV/s. Ferrocene was added to recalibrate the curves. Potential are given versus SCE.

5. SEM images of the fullerene-based compact layers.

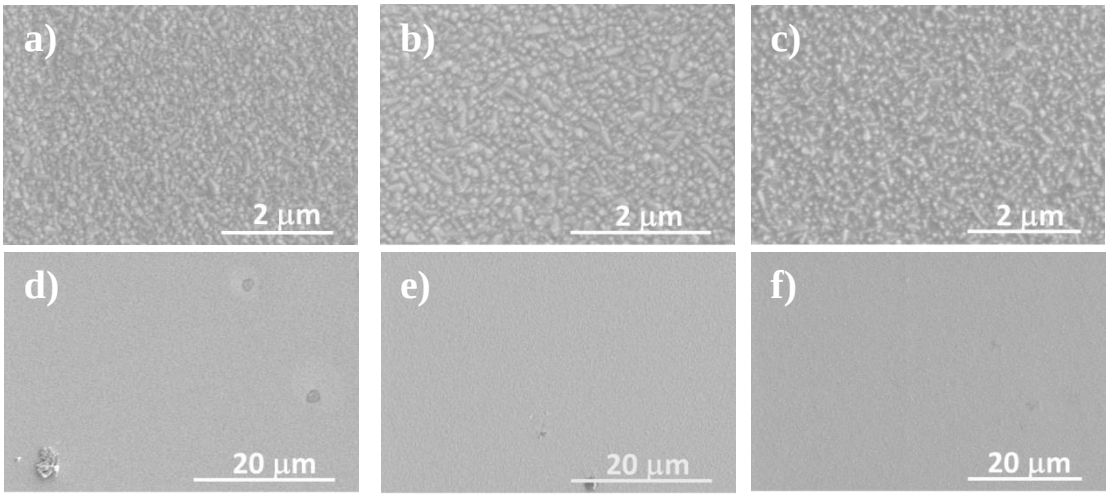

Figure S8. SEM images of **(a,d)** sol-gel C_{60} after cross-linking, **(b,e)** PCBCB after cross-linking, and **(c,f)** C_{60} films, processed on FTO glass.

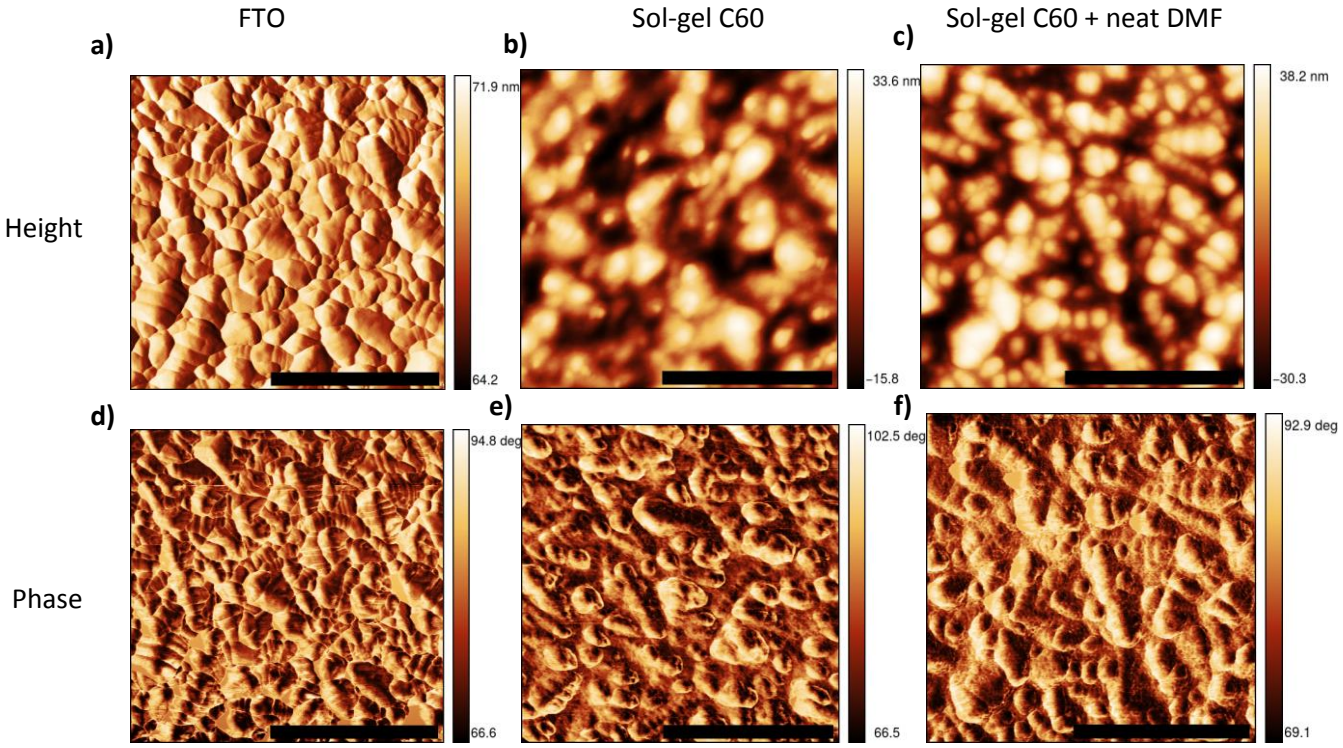

Figure S9. AFM topography (1x1μm^2) and phase images of bare FTO (a, d) , sol-gel C_{60} films (b, e) before the application of solvent and after spin-coating DMF (c,f) and acquired with an Asylum Instruments MFP-3D.

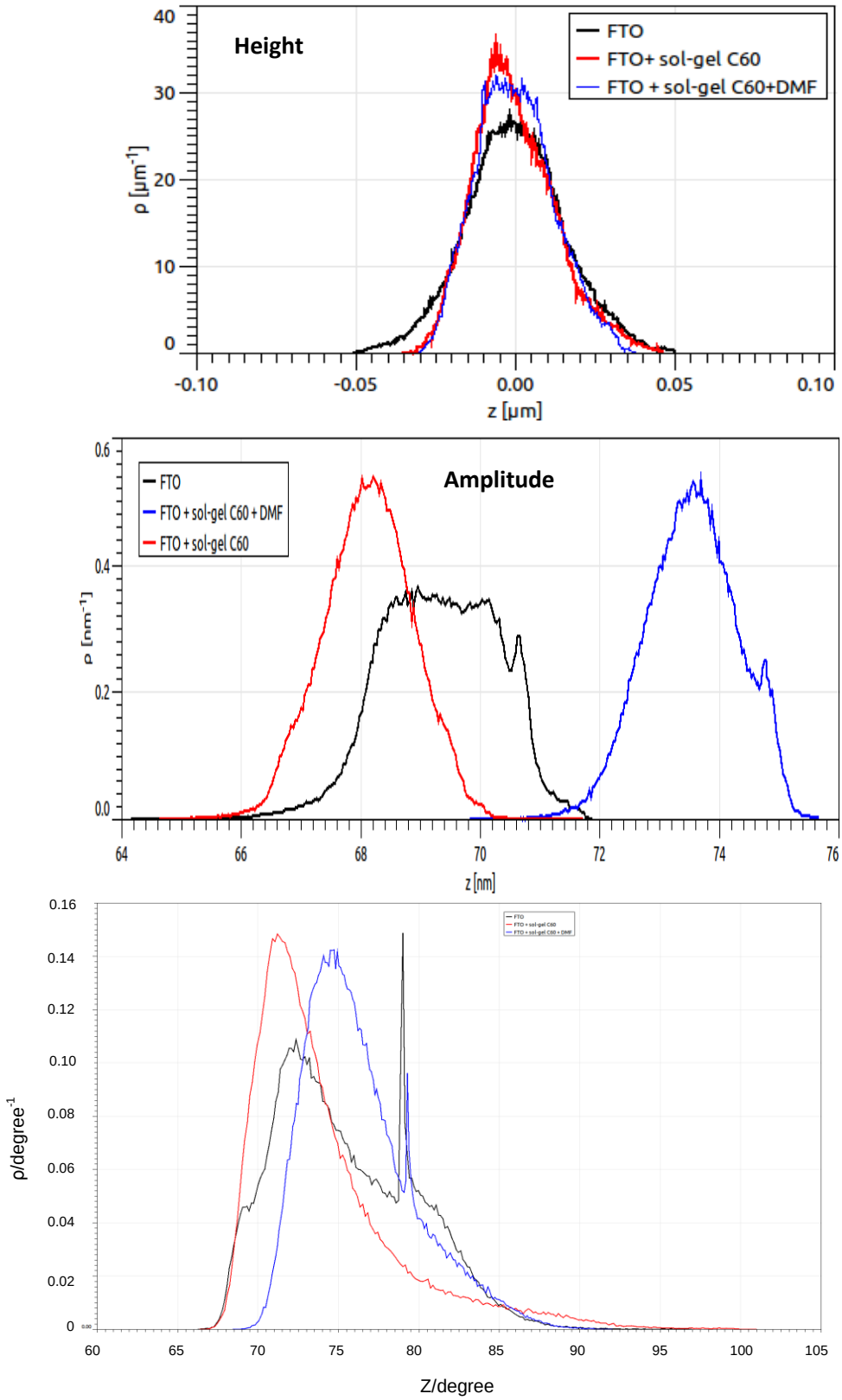

Figure S10. Histograms corresponding to the scans presented in figure S10.

6. SEM images of the perovskite films processed on different fullerene layers

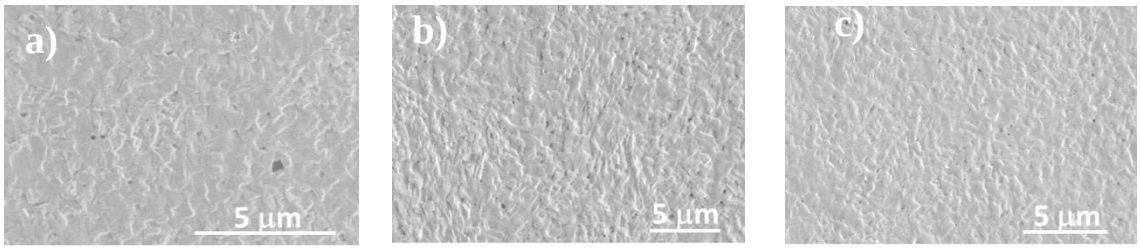

Figure S11. SEM images of perovskite films grown on **(a)** sol-gel C_{60}, **(b)** PCBCB, and **(c)** C_{60} layer.

7. SCLC data

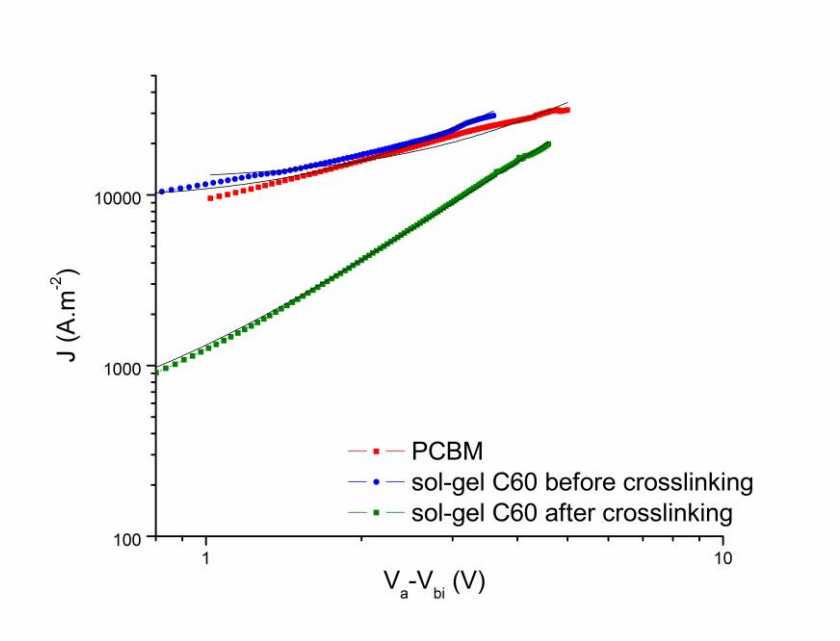

Figure S12. SCLC data and fits for the sol-gel. See methods section for fitting procedure and device architecture.

REFERENCES

((1) Lee, M. M.; Teuscher, J.; Miyasaka, T.; Murakami, T. N.; Henry, J. Efficient Hybrid Solar Cells Based on Meso-Superstructured Organometal Halide Perovskites. *Science.* **2012**, *338*, 643–647.

(2) Deb, N.; Dasari, R. R.; Moudgil, K.; Hernandez, J. L.; Marder, S. R.; Sun, Y.; Karim, A.; Bucknall, D. G. Thermo-Cross-Linkable Fullerene for Long-Term Stability of Photovoltaic Devices. *J. Mater. Chem. A* **2015**, *3*, 21856–21863.

(3) Eperon, G. E.; Burlakov, V. M.; Docampo, P.; Goriely, A.; Snaith, H. J. Morphological Control for High Performance, Solution-Processed Planar Heterojunction Perovskite Solar Cells. *Adv. Funct. Mater.* **2013**, *24*, 151.

(4) Abate, A.; Saliba, M.; Hollman, D. J.; Stranks, S. D.; Wojciechowski, K.; Avolio, R.; Grancini, G.; Petrozza, A.; Snaith, H. J. Supramolecular Halogen Bond Passivation of Supramolecular Halogen Bond Passivation of Organic-Inorganic Halide Perovskite Solar Cells. *Nano Lett.* **2014**, *14*, 3247–3254.

(5) Noel, N. K.; Abate, A.; Stranks, S. D.; Parrott, E. S.; Burlakov, V. M.; Goriely, A.; Snaith, H. J. Enhanced Photoluminescence and Solar Cell Performance via Lewis Base Passivation of Organic-Inorganic Lead Halide Perovskites. *ACS Nano* **2014**, *8*, 9815–9821.

(6) Nečas, D.; Klapetek, P. Gwyddion: An Open-Source Software for SPM Data Analysis. *Open Phys.* **2012**, *10* (1).